

A general and very straightforward route to the selective N-functionalization of 1,4,7-triazacyclononane with imidazole groups. Crystal structure determinations of nickel(II), copper(II) and zinc(II) complexes

Massimo Di Vaira *, Fabrizio Mani, Piero Stoppioni

Dipartimento di Chimica, Università di Firenze, via Maragliano 77, 50144 Florence, Italy

Received 5 July 1999; accepted 22 October 1999

Abstract

An easy, one-step procedure for the synthesis of the selectively substituted macrocycles 1-(1-methylimidazol-2-ylmethyl)-1,4,7-triazacyclononane, L^1 , and 1,4-bis(1-methylimidazol-2-ylmethyl)-1,4,7-triazacyclononane, L^2 , is reported. The potentially tetra-, L^1 , and pentadentate, L^2 , compounds yield nickel(II), copper(II) and zinc(II) complexes which have been isolated in the solid state. The crystal structures of $[\text{NiL}^1(\text{N}_3)]_2[\text{PF}_6]_2$ (**1**), $[\text{Cu}_2\text{L}^2(\text{OH})][\text{PF}_6]_3$ (**2**), $[\text{ZnL}^1\text{Cl}][\text{BPh}_4]$ (**3**), $[\text{NiL}^2(\text{H}_2\text{O})][\text{BPh}_4]_2 \cdot \text{C}_2\text{H}_5\text{OH}$ (**4**) and $[\text{Ni}_2\text{L}^2(\text{N}_3)][\text{PF}_6]_3$ (**5**) have been determined by X-ray diffraction studies. The L^1 and L^2 molecules provide four and, respectively, five nitrogens for complexation of the metal ions whose coordination requirements are completed by additional ligands either terminal (Cl, H_2O , compounds **3** and **4**) or bridging two metal ions (N_3^- , compounds **1** and **5**; OH^- , compound **2**). In its complexes nickel(II) is six-coordinated in an approximately octahedral environment. Both copper(II) and zinc(II) are five-coordinated with geometries approximately square pyramidal and, respectively, trigonal bipyramidal. © 2000 Elsevier Science S.A. All rights reserved.

Keywords: Crystal structures; Nickel complexes; Copper complexes; Zinc complexes; Aza macrocycle complexes

1. Introduction

We are interested in the synthesis of ligands through the functionalization of 1,4,7-triazacyclononane ($[\text{9}]_{\text{ane}}\text{N}_3$) with pendant donor groups of different nature, in order to improve the selectivity of the ligands and the stability of the complexes [1]. To that purpose mono- and di-functionalized derivatives of $[\text{9}]_{\text{ane}}\text{N}_3$ have to be readily available in high yields. While a large number of hexadentate compounds derived from N-functionalization of $[\text{9}]_{\text{ane}}\text{N}_3$ with three identical pendant groups have recently been reported [2,3], selectively N-functionalized compounds are comparatively rare [4]. This reveals the difficulties encountered for the attachment of only one or two pendant groups

to the polyazamacrocycle according to multistep processes with low yields. Our interest in this field prompted us to exploit a variety of alternative synthetic methods to selectively functionalize polyazamacrocycles and some time ago we reported the synthesis of 1,4-bis(1-methylimidazol-2-ylmethyl)-1,4,7-triazacyclononane with the use of 1,8-bis-(dimethylamino)-naphthalene (Proton Sponge[®]) as the base [1,5]. Now we have devised an improved and efficient strategy which allows to obtain mono- and di-functionalized $[\text{9}]_{\text{ane}}\text{N}_3$ with remarkable synthetic simplicity and in high yields. From these compounds it is possible to obtain unsymmetrically functionalized macrocycles by means of routine organic procedures.

In this paper we describe the one-step synthesis of the two compounds 1-(1-methylimidazol-2-ylmethyl)-1,4,7-triazacyclononane, L^1 , and 1,4-bis(1-methylimidazol-2-ylmethyl)-1,4,7-triazacyclononane, L^2 . The coordination properties of the two ligands have been inves-

* Corresponding author. Tel.: +39-055-321 631; fax: +39-055-354 845.

tigated towards some 3d metal ions and the X-ray structure determinations of the complexes $[\text{NiL}^1(\text{N}_3)]_2\text{-}[\text{PF}_6]_2$ (**1**), $[\text{Cu}_2\text{L}_2^1(\text{OH})][\text{PF}_6]_3$ (**2**), $[\text{ZnL}^1\text{Cl}]\text{BPh}_4$ (**3**), $[\text{NiL}^2(\text{H}_2\text{O})][\text{BPh}_4]_2\cdot\text{C}_2\text{H}_5\text{OH}$ (**4**) and $[\text{Ni}_2\text{L}_2^2(\text{N}_3)][\text{PF}_6]_3$ (**5**) have been carried out.

2. Experimental

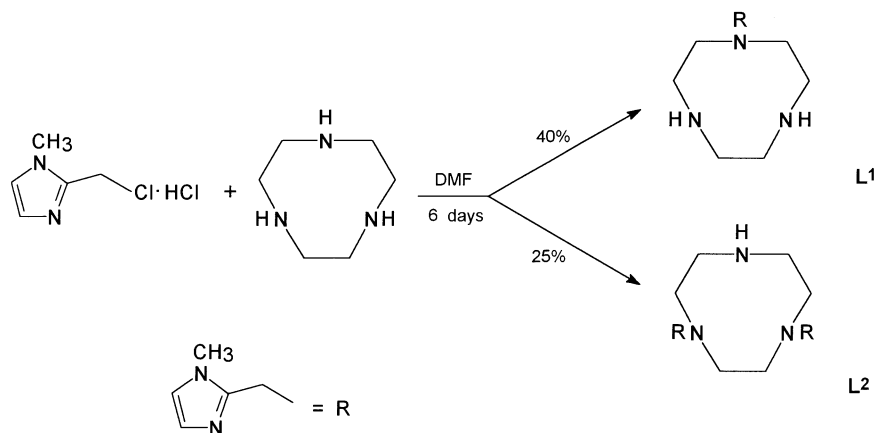
2.1. Materials and methods

All reagents were reagent grade; commercial solvents, when required by the synthetic procedures, were dried according to standard methods and distilled just before their use. Hydrated zinc perchlorate was prepared using a standard procedure. The intermediate compounds 1,4,7-triazacyclononane [6] and 2-chloromethyl-1-methylimidazole [7] were prepared according to published procedures. The purity of the products was checked by means of ^{13}C NMR, verifying that the spectra exhibited the expected resonances. Hydrated metal(II) chlorides, hydrated $\text{CuCO}_3\cdot\text{Cu}(\text{OH})_2$, NaBPh_4 , TIPF_6 and NaN_3 are commercially available and were used as received. Elemental analyses were performed by the Microanalytical Laboratory of the Department of Chemistry of the University of Florence. The ^{13}C NMR spectra of the compounds were obtained with a Varian FT 80 spectrometer operating at 20.0 MHz. Infrared spectra were recorded with a Perkin–Elmer 283 grating spectrophotometer as Nujol mulls between KBr plates; electronic spectra were recorded in the range 300–2000 nm with a Perkin–Elmer Lambda 9 spectrophotometer; the concentration of the solutions was ca. 1.0×10^{-3} M.

2.2. Syntheses of the ligands

The procedure for the synthesis of the ligands is outlined in Scheme 1. The reactions were carried out

under a N_2 atmosphere using deaerated solvents. Solid 2-chloromethyl-1-methylimidazole hydrochloride (13.5 g, 0.0808 mol) was slowly added to a solution of 1,4,7-triazacyclononane (10.0 g, 0.0775 mol) in dry DMF (400 ml). The reactants were stirred at room temperature for 6 days, during which increasing amounts of a solid compound formed. The solid compound was separated from the solution by filtration under N_2 , washed with an ethanol–diethyl ether mixture (50–50 by volume), then with diethyl ether alone, and was finally dried in a stream of N_2 at about 40°C . This compound is the bis-hydrochloride of 1-(1-methylimidazol-2-ylmethyl)-1,4,7-triazacyclononane, L^1 , in fairly pure form. Yield (average) 9.2 g, 40%. The purity of the compound was checked by means of ^{13}C NMR, verifying that the spectra exhibited the expected resonances. ^{13}C NMR (D_2O): δ 145.0 (C^2 of imidazole), 123.4, 121.6 (C^4 , C^5 of imidazole), 48.7 (bridge- CH_2), 43.8, 42.5, 42.3 (CH_2 of macrocycle), 33.3 (CH_3 of imidazole). The DMF solution was rotary evaporated to dryness, the resulting solid was dissolved in water and the pH of the solution was adjusted to 9 with NaOH . The water solution was extracted with CHCl_3 (30 ml) in order to remove possible traces of unreacted $[\text{9}]_3\text{aneN}_3$ and 2-chloromethyl-1-methylimidazole. The water solution was made strongly basic with NaOH and extracted two times with CHCl_3 (50 ml each). After drying the CHCl_3 layer with anhydrous sodium sulfate, rotary evaporation to dryness gave a crude product in oily form which was found to contain 1,4-bis(1-methylimidazol-2-ylmethyl)-1,4,7-triazacyclononane, L^2 , and traces of the monosubstituted compound L^1 and of unreacted $[\text{9}]_3\text{aneN}_3$. Yield (average) 6.1 g, 25%. For its purification, the crude product was dissolved in CHCl_3 and eluted through a neutral alumina column (Aldrich, type 507 C, 150 mesh) with a chloroform–methanol mixture (95–5 by volume). ^{13}C NMR (D_2O): δ 146.7 (C^2 of imidazole), 126.6, 123.3 (C^4 , C^5 of imidazole), 53.3 (bridge- CH_2), 52.1, 50.5, 45.2 (CH_2 of macrocycle), 33.2 (CH_3 of imidazole).



Scheme 1.

2.3. Syntheses of the complexes

2.3.1. $[\text{NiL}^1(\text{N}_3)]_2[\text{PF}_6]_2$ (**1**)

Solutions of hydrated NiCl_2 (238 mg, 1.0 mmol) in EtOH (20 ml), of $\text{L}^1\cdot 2\text{HCl}$ (296 mg, 1.0 mmol) in MeOH (30 ml) and of NaN_3 (65 mg, 1.0 mmol) in H_2O (20 ml) were mixed at boiling temperature. To the resulting solution, solid Na_2CO_3 (200 mg) in excess to the stoichiometric ratio was added followed by an acetone solution (30 ml) of TIPF_6 (349 mg, 1.0 mmol). The suspension was stirred at 40°C for 10 min, cooled to room temperature and filtered to remove solid TiCl . Finally, the solution was concentrated to a small volume until a lilac crystalline compound was obtained. Slow evaporation at room temperature of a MeCN – EtOH solution of the compound gave the crystals used for X-ray analysis. Calc. for $\text{C}_{22}\text{H}_{42}\text{F}_{12}\text{N}_{16}\text{Ni}_2\text{P}_2$: C, 28.2; H, 4.52; N, 23.9. Found: C, 28.6; H, 4.64; N, 24.0%. UV–Vis (λ_{max} (nm); ϵ ($\text{cm}^2 \text{mmol}^{-1}$): diffuse reflectance 310, 560, 850(sh), 920; CH_3CN solution 300(810), 560(15), 820(sh), 920(26). IR (KBr, ν (cm^{-1})), 2075, $\nu(\text{N}_3)$.

2.3.2. $[\text{Cu}_2\text{L}_2^1(\text{OH})][\text{PF}_6]_3$ (**2**)

Solid $\text{CuCO}_3\cdot\text{Cu}(\text{OH})_2\cdot n\text{H}_2\text{O}$ (110 mg, ca. 0.5 mmol) was added to a boiling solution in EtOH (50 ml) of $\text{L}^1\cdot 2\text{HCl}$ (296 mg, 1.0 mmol). After dissolution of the copper compound, a water solution of Na_2CO_3 (106 mg, 1.0 mmol) and an acetone solution (20 ml) of TIPF_6 (698 mg, 2.0 mmol) were added in the order to the reactant solution. The suspension was stirred for 10 min at 40°C , cooled to room temperature and filtered to remove solid TiCl . Slow evaporation of the solution gave a blue crystalline compound. Crystals suitable for X-ray analysis were grown from a MeCN – EtOH solution of the compound. Calc. for $\text{C}_{22}\text{H}_{43}\text{Cu}_2\text{F}_{18}\text{N}_{10}\text{OP}_3$: C, 25.8; H, 4.23; N, 13.6. Found: C, 25.8; H, 4.36; N, 13.6%. UV–Vis (λ_{max} (nm); ϵ ($\text{cm}^2 \text{mmol}^{-1}$): diffuse reflectance 610, 700(sh), 950; CH_3CN solution 630(120), 970(27).

2.3.3. $[\text{ZnL}^1\text{Cl}]\text{BPh}_4$ (**3**)

Warm solutions of hydrated $\text{Zn}(\text{ClO}_4)_2$ (372 mg, 1.0 mmol) in EtOH (20 ml) and of $\text{L}^1\cdot 2\text{HCl}$ (296 mg, 1.0 mmol) in MeOH (20 ml) were mixed and solid Na_2CO_3 (159 mg, 1.5 mmol) was added to the resulting solution. The suspension was allowed to boil for 10 min and filtered to remove unreacted Na_2CO_3 . Then NaBPh_4 (342 mg, 1.0 mmol) dissolved in acetone (30 ml) was added to the resulting solution. The solution was concentrated until a white crystalline compound was obtained which was recrystallized from a Me_2CO – EtOH mixture. Calc. for $\text{C}_{35}\text{H}_{41}\text{BClN}_5\text{Zn}$: C, 65.3; H, 6.42; N, 10.9. Found C, 65.0; H, 6.79; N, 10.6%. The complex is scarcely soluble in the common deuterated solvents.

2.3.4. $[\text{NiL}^2(\text{H}_2\text{O})][\text{BPh}_4]_2\cdot\text{C}_2\text{H}_5\text{OH}$ (**4**)

A solution of hydrated NiCl_2 (238 mg, 1.0 mmol) and of L^2 (317 mg, 1.0 mmol) in EtOH (40 ml) and a solution of NaBPh_4 (684 mg, 2.0 mmol) in acetone (20 ml) were mixed together at boiling temperature and concentrated until a lilac crystalline compound was obtained. Recrystallization of the compound from a Me_2CO – EtOH mixture gave the crystals used for X-ray analysis. Calc. for $\text{C}_{66}\text{H}_{75}\text{B}_2\text{N}_7\text{NiO}_2$: C, 73.5; H, 7.01; N, 9.09. Found: C, 73.5; H, 7.11; N, 9.12%. UV–Vis (λ_{max} (nm); ϵ ($\text{cm}^2 \text{mmol}^{-1}$): diffuse reflectance 330, 540, 800(sh), 870; CH_3CN solution: 340(29), 540(20), 800(sh), 870(25).

2.3.5. $[\text{Ni}_2\text{L}_2^2(\text{N}_3)][\text{PF}_6]_3$ (**5**)

This compound was prepared by the same procedure as compound **1** but using L^2 instead of $\text{L}^1\cdot 2\text{HCl}$ and without addition of Na_2CO_3 . Calc. for $\text{C}_{32}\text{H}_{54}\text{F}_{18}\text{N}_{17}\text{Ni}_2\text{P}_3$: C, 31.3; H, 4.44; N, 19.4. Found: C, 31.4; H, 4.50; N, 19.3%. UV–Vis (λ_{max} (nm); ϵ ($\text{cm}^2 \text{mmol}^{-1}$): diffuse reflectance 330, 540, 800(sh), 890; CH_3CN solution: 349(29), 540(20), 800(sh), 870(25). IR (KBr, ν (cm^{-1})), 2080, $\nu(\text{N}_3)$.

2.3.6. $[\text{CuL}^2][\text{PF}_6]_2$ (**6**)

Warm solutions of hydrated CuCl_2 (170 mg, 1.0 mmol), of L^2 (317 mg, 1.0 mmol) in EtOH (40 ml) and of TIPF_6 (698 mg, 2.0 mmol) in acetone (30 ml) were mixed together and the suspension was stirred at 40°C for 10 min. Afterward the suspension was cooled to room temperature, TiCl discarded by filtration and the resulting solution was concentrated until a blue crystalline compound was obtained. Recrystallization was carried out with a MeCN – EtOH mixture. Calc. for $\text{C}_{16}\text{H}_{27}\text{CuF}_{12}\text{N}_7\text{P}_2$: C, 28.6; H, 4.10; N, 14.6. Found C, 28.7; H, 4.20; N, 14.5%. UV–Vis (λ_{max} (nm); ϵ ($\text{cm}^2 \text{mmol}^{-1}$): diffuse reflectance 380(sh) 610, 960; CH_3CN solution: 380(sh), 620(145), 970(30).

2.3.7. $[\text{ZnL}^2][\text{ClO}_4]_2$ (**7**)

The solution of hydrated $\text{Zn}(\text{ClO}_4)_2$ (372 mg, 1.0 mmol) and L^2 (317 mg, 1.0 mmol) in EtOH (40 ml) was concentrated until a white crystalline product was obtained which was recrystallized from water. Calc. for $\text{C}_{16}\text{H}_{27}\text{Cl}_2\text{N}_7\text{O}_8\text{Zn}$: C, 33.0; H, 4.69; N, 16.8. Found: C, 33.3; H, 4.91; N, 16.7%. ^{13}C NMR (D_2O): δ 146.6 (C^2), 123.9, 123.7 (C^4 , C^5), 52.9, 51.7, 51.4, 43.4 (unresolved CH_2), 32.0 (CH_3 of imidazole).

2.4. X-ray data collections, structure determinations and refinements

X-ray diffraction data were collected for the compounds $[\text{NiL}^1(\text{N}_3)]_2[\text{PF}_6]_2$ (**1**), $[\text{Ni}_2\text{L}_2^2(\text{N}_3)][\text{PF}_6]_3$ (**5**), $[\text{NiL}^2(\text{H}_2\text{O})][\text{BPh}_4]_2\cdot\text{C}_2\text{H}_5\text{OH}$ (**4**), $[\text{Cu}_2\text{L}_2^1(\text{OH})][\text{PF}_6]_3$ (**2**) and $[\text{ZnL}^1\text{Cl}]\text{BPh}_4$ (**3**) at room temperature on a

Table 1
 Crystallographic data for $[\text{NiL}^1(\text{N}_3)]_2[\text{PF}_6]_2$ (**1**), $[\text{Ni}_2\text{L}_2^2(\text{N}_3)][\text{PF}_6]_3$ (**5**), $[\text{NiL}^2(\text{H}_2\text{O})][\text{BPh}_4]_2 \cdot \text{C}_2\text{H}_5\text{OH}$ (**4**), $[\text{Cu}_2\text{L}_2^1(\text{OH})][\text{PF}_6]_3$ (**2**) and $[\text{ZnL}^1\text{Cl}][\text{BPh}_4]$ (**3**)

	1	5	4	2	3
Formula	$\text{C}_{22}\text{H}_{42}\text{F}_{12}\text{N}_{16}\text{Ni}_2\text{P}_2$	$\text{C}_{32}\text{H}_{54}\text{F}_{18}\text{N}_{17}\text{Ni}_2\text{P}_3$	$\text{C}_{66}\text{H}_{75}\text{B}_2\text{N}_7\text{NiO}_2$	$\text{C}_{22}\text{H}_{43}\text{Cu}_2\text{F}_{18}\text{N}_{10}\text{OP}_3$	$\text{C}_{35}\text{H}_{41}\text{BClN}_5\text{Zn}$
<i>M</i>	938.08	1229.25	1078.66	1025.65	643.36
Crystal system	monoclinic	monoclinic	triclinic	orthorhombic	monoclinic
Space group	<i>C2/c</i> (no. 15)	<i>C2/c</i> (no. 15)	<i>P</i> $\bar{1}$ (no. 2)	<i>P2₁nb</i> (no. 33)	<i>P2₁/n</i> (no. 14)
<i>a</i> (Å)	25.642(1)	18.776(3)	11.021(6)	10.762(2)	9.335(4)
<i>b</i> (Å)	11.651(1)	18.993(4)	13.581(4)	17.019(4)	21.755(6)
<i>c</i> (Å)	13.168(2)	15.884(6)	19.606(8)	20.265(5)	16.175(4)
α (°)	90.00	90.00	96.45(3)	90.00	90.00
β (°)	113.93(1)	118.36(3)	91.06(4)	90.00	96.40(3)
γ (°)	90.00	90.00	96.14(3)	90.00	90.00
<i>U</i> (Å ³)	3595.8(6)	4985(2)	2898(2)	3712(1)	3264(2)
<i>Z</i>	4	4	2	4	4
<i>D_c</i> (g cm ⁻³)	1.733	1.638	1.236	1.835	1.309
Crystal size (mm)	0.20 × 0.25 × 0.40	0.17 × 0.33 × 0.70	0.15 × 0.40 × 0.60	0.10 × 0.25 × 0.50	0.50 × 0.60 × 0.70
μ (mm ⁻¹)	3.12	0.966	0.386	3.83	0.866
Radiation	Cu K α ($\lambda = 1.5418$ Å)	Mo K α ($\lambda = 0.71069$ Å)	Mo K α ($\lambda = 0.71069$ Å)	Cu K α ($\lambda = 1.5418$ Å)	Mo K α ($\lambda = 0.71069$ Å)
Data collected ^a	$\pm h, +k, +l$	$\pm h, +k, +l$	$\pm h, \pm k, +l$	redundant	$\pm h, +k, +l$
Scan type	ω -2 θ	ω -2 θ	ω -2 θ	ω	ω -2 θ
2 θ range (°)	7–140	5–50	5–45	7–113	5–52
Reflections collected	3919	4567	7491	13924	7141
Unique reflections	3198	4386	7491	4196	6070
Unique observed reflections, with $I > 2\sigma(I)$	3086	3276	4379	3932	4409
Absorption correction	ψ scan method	no	empirical, DIFABS	empirical, SADABS	no
No. parameters	247	328	725	507	478
<i>R</i> ₁ (observed reflections)	0.051	0.051	0.081	0.053	0.046
<i>R</i> ₁ (all unique reflections)	0.052	0.077	0.157	0.056	0.080
<i>wR</i> ₂	0.138	0.146	0.222	0.146	0.136
Goodness-of-fit	1.076	1.037	1.063	1.057	1.028
Largest features (max, min) in final ΔF map (e Å ⁻³)	0.83, -0.53	0.55, -0.38	0.49, -0.42	0.55, -0.54	0.67, -0.50

^a Data collections performed with P4 (**1**), CAD4 (**5**, **4** and **3**) and CCD (**2**) instruments.

Bruker-AXS P4 diffractometer (**1**) using graphite-monochromated Cu K α radiation, on an Enraf-Nonius CAD4 diffractometer (**5**, **4** and **3**) with graphite-monochromated Mo K α radiation, and on a Bruker-AXS CCD platform (**2**) with Cu K α radiation from a rotating anode generator equipped with Göbel mirrors. Crystal data and details about data collection and structure refinements are given in Table 1. Unit-cell parameters were obtained from the settings of 30 reflections with $20 < \theta < 30^\circ$ (**1**), of 24 reflections with $15 < \theta < 16^\circ$ (**5**), $13 < \theta < 15^\circ$ (**4**) and $13 < \theta < 16^\circ$ (**3**), and of 6069 reflections with $3 < \theta < 56^\circ$ (**2**). No crystal decay was observed during data collections. Empirical corrections for absorption based on ψ scans (**1**) or using DIFABS [8] (**4**) or SADABS [9] (**2**) were applied, but no corrections were applied for **5** and **3**, for which ψ scan data were not available and DIFABS failed to yield significant improvements. A small correction for extinction effects had to be applied to the data of **1**. The main programs used in the crystallographic calculations are listed in Refs. [8–13].

The structures were solved by direct (SIR [10]) and heavy-atom (SHELXL 93 [11]) methods and were refined by full-matrix least-squares on F_o^2 . In the final refinement cycles on all structures the non-hydrogen atoms, including the fractional atoms of the solvent in **4** (see below) were assigned anisotropic temperature factors. The positional parameters of the hydrogen atoms of the water molecule in **4** were refined with one geometrical restraint; also those of most hydrogens in **3** were refined with three separate and soft restraints for the N–H, the aromatic and the aliphatic hydrogens of the dangling group of L¹. The hydrogens of the macrocyclic ring of **3**, whose sites were affected by relatively high thermal motion, all the hydrogen atoms in **4** (except those of the H₂O molecule) as well as those of the other structures were in calculated positions, riding on the carrier atoms (methyls being treated as rigid groups). In all cases the H temperature factors were assigned according to the expression $U_{\text{H}} = 1.2U_{\text{C}}^{\text{eq}}$ ($U_{\text{H}} = 1.5U_{\text{C}}^{\text{eq}}$ for methyl hydrogens). A soft restraint was imposed on the C–C

distances of the phenyl groups in **4**. The ethanol solvate molecule in the same structure, affected by disorder, was refined as being distributed between two orientations with fixed complementary population parameters, assigned on the basis of refinement cycles performed with an overall temperature factor for all the fractional sites of the solvent model. Common restraints were imposed on corresponding bond distances in the two fractions of the ethanol molecule; the short C–C value obtained should be attributed to effects of thermal motion and/or disorder. The absolute configuration for the acentric structure of **2** could not be assigned on the basis of Flack's test [14], probably due to the small anomalous dispersion effects for this compound with Cu K α radiation (actually, the absolute configuration could be assigned for a different crystal of **2**, based on Mo K α data collected on the CAD4 instrument; those data, however, were considered to be of overall worse quality than the present ones).

3. Results and discussion

The selectively substituted macrocycles 1-(1-methylimidazol-2-ylmethyl)-1,4,7-triazacyclononane, **L**¹, obtained as the bis-hydrochloride salt, and 1,4-bis-(1-methylimidazol-2-ylmethyl)-1,4,7-triazacyclononane, **L**², were prepared by a very simple one-step procedure which involves the reaction of 2-chloromethyl-1-methylimidazole hydrochloride with 1,4,7-triazacyclononane in a molar ratio close to 1:1. The synthetic route is summarized in Scheme 1. The reactants in DMF were allowed to react for 6 days at room temperature; then the **L**¹ ligand was separated from the reaction mixture as the bis-hydrochloride in fairly pure form and in good yield. After removal of the solid **L**¹·2HCl from the DMF solution, the **L**² ligand was recovered as a byproduct by means of standard workup. The purity of the ligands was checked by means of their ¹³C NMR spectra in D₂O. In the above synthetic procedure the macrocycle to be functionalized acts as the base and the protonation of the secondary amines of the macrocycle prevents their functionalization. The molar ratio of the two reactants, the choice of the solvent and the temperature and the extent of the reaction time were found to be crucial factors for the success of the synthesis. The experimental conditions reported (see Section 2) are those which gave the best yields of **L**¹ and **L**² (65% overall with respect to [9]aneN₃).

The complexes were prepared by the reactions of compounds **L**¹·2HCl or **L**² and the appropriate metal(II) salts in EtOH–MeOH mixtures. The syntheses of the complexes with **L**¹·2HCl require a basic medium. Even if the ligands have potentially deprotonable NH

groups, in no case such deprotonation occurred upon reaction with the Ni(II), Cu(II) and Zn(II) salts even in basic conditions, as shown by the stoichiometries of the complexes obtained. Moreover the IR spectra of the complexes exhibit strong absorptions in the 3200–3280 region due to N–H stretching. The **L**¹ and **L**² compounds provide four and, respectively, five nitrogen donors for complexation of the metal ions thus favouring the binding of additional ligands to the [ML]²⁺ (**L** = **L**¹, **L**²) moieties in order to satisfy the coordination requirements of the metal ions, which generally exceed the denticities of both ligands.

The nickel(II) compounds have the formulae NiL¹N₃PF₆ (**1**), NiL²H₂O(BPh₄)₂·C₂H₅OH (**4**) and Ni₂(L²)₂N₃(PF₆)₃ (**5**). Their electronic spectra recorded on the solid samples and in MeCN solutions are all indicative of a six-coordinate environment of high-spin nickel(II). In particular, the marked splitting of the low-energy band at 800–900 nm is typical of trigonally distorted symmetry [15]. In the nickel complexes **1** and **5** the ligands block four (**L**¹) and five (**L**²) coordination sites of an octahedral environment thus leaving sites available for possible N₃[−] coordination. The stoichiometry of the copper(II) complex Cu₂(L¹)₂(OH)(PF₆)₃ suggests a dinuclear structure with one bridging hydroxide and a five-coordinate metal environment. Comparison of the electronic spectra of the solid compound and of its MeCN solution suggests that the dinuclear structure is disrupted in solution where the hydroxide ion is most likely replaced by a solvent molecule. The ¹³C NMR spectrum of ZnL²(ClO₄)₂ in D₂O exhibits one resonance from each group of chemically equivalent carbon atoms suggesting that only a single symmetric species, presumably five-coordinate, is present in solution. The ZnL¹CIBPh₄ complex is not sufficiently soluble in the common deuterated solvents to give meaningful ¹³C NMR spectra.

In the structures of the nickel compounds each of the metal atoms is six-coordinated in an approximately octahedral environment, being surrounded by all the donor atoms of the substituted macrocyclic ligand and by N₃[−] nitrogen or water oxygen atoms. In each case the three macrocycle nitrogens span one face of the octahedron about the metal atom forming N–Ni–N angles < 90°. This may be at the origin of the trigonal distortion suggested by the electronic spectra of the compounds.

The dimeric [NiL¹(N₃)₂]²⁺ cation of **1** (Fig. 1 and Table 2) possesses a twofold symmetry axis normal to the N₃[−] anions, which are substantially parallel to each other and bridge the two metal atoms. Two N₃[−] nitrogens and the methylimidazole donor atom define the face of the octahedron about the nickel atom lying *trans* to the face occupied by the macrocycle nitrogens. Probably due to the effects of packing forces, the two

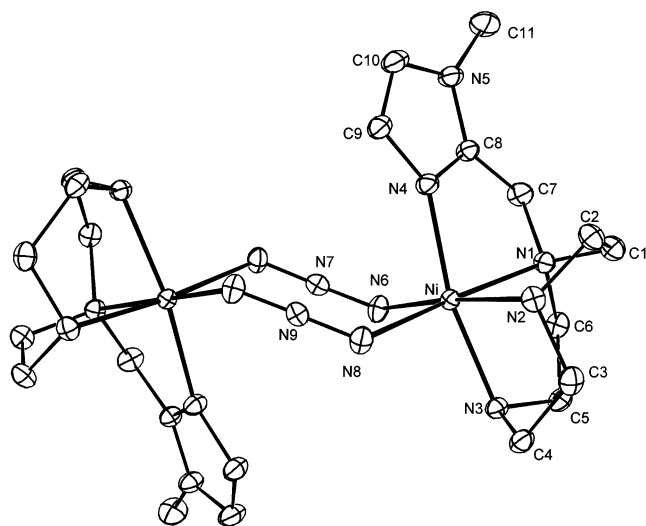


Fig. 1. A view of the dimeric $[\text{NiL}^1(\text{N}_3)]_2^{2+}$ cation in the structure of **1**, showing the atom numbering scheme for the symmetry independent part of the cation. A twofold axis passes through atoms N(7) and N(9).

Table 2
Selected bond lengths (Å) and angles (°) for $[\text{NiL}^1(\text{N}_3)]_2[\text{PF}_6]_2$ (**1**)

Ni–N(1)	2.126(2)	Ni–N(6)	2.153(3)
Ni–N(2)	2.083(3)	Ni–N(8)	2.086(3)
Ni–N(3)	2.084(3)	N(6)–N(7)	1.175(3)
Ni–N(4)	2.051(3)	N(8)–N(9)	1.169(3)
N(1)–Ni–N(2)	83.38(10)	N(3)–Ni–N(4)	164.36(11)
N(1)–Ni–N(3)	83.51(10)	N(3)–Ni–N(6)	91.40(11)
N(1)–Ni–N(4)	80.96(10)	N(3)–Ni–N(8)	95.26(11)
N(1)–Ni–N(6)	94.12(11)	N(4)–Ni–N(6)	87.87(12)
N(1)–Ni–N(8)	174.45(10)	N(4)–Ni–N(8)	100.37(11)
N(2)–Ni–N(3)	83.01(11)	N(6)–Ni–N(8)	91.32(12)
N(2)–Ni–N(4)	97.00(11)	Ni–N(6)–N(7)	121.0(2)
N(2)–Ni–N(6)	174.09(11)	Ni–N(8)–N(9)	122.7(2)
N(2)–Ni–N(8)	91.10(11)		

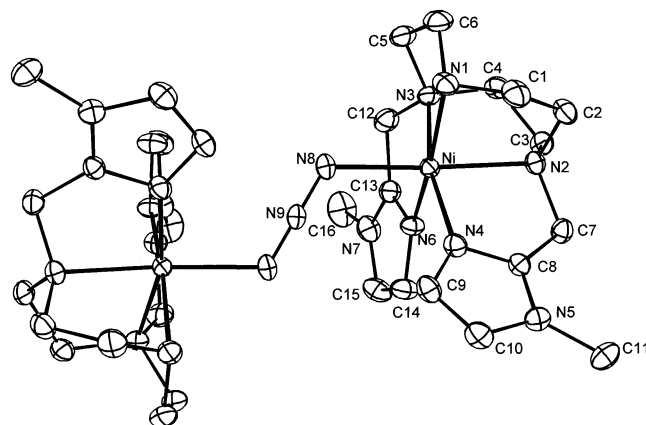


Fig. 2. A view of the dimeric $[\text{Ni}_2\text{L}_2^2(\text{N}_3)]^{3+}$ cation in the structure of **5**. Atom N(9) lies on a twofold axis. Only atoms forming the asymmetric unit are labelled.

Table 3
Selected bond lengths (Å) and angles (°) for $[\text{Ni}_2\text{L}_2^2(\text{N}_3)][\text{PF}_6]_3$ (**5**)

Ni–N(1)	2.080(4)	Ni–N(6)	2.059(4)
Ni–N(2)	2.111(3)	Ni–N(8)	2.095(4)
Ni–N(3)	2.122(4)	N(8)–N(9)	1.169(4)
Ni–N(4)	2.048(4)		
N(1)–Ni–N(2)	83.31(14)	N(2)–Ni–N(8)	174.2(2)
N(1)–Ni–N(3)	83.9(2)	N(3)–Ni–N(4)	165.34(13)
N(1)–Ni–N(4)	99.3(2)	N(3)–Ni–N(6)	79.93(14)
N(1)–Ni–N(6)	163.8(2)	N(3)–Ni–N(8)	96.4(2)
N(1)–Ni–N(8)	91.1(2)	N(4)–Ni–N(6)	96.7(2)
N(2)–Ni–N(3)	84.57(13)	N(4)–Ni–N(8)	97.8(2)
N(2)–Ni–N(4)	81.64(13)	N(6)–Ni–N(8)	89.2(2)
N(2)–Ni–N(6)	96.63(14)	Ni–N(8)–N(9)	119.5(3)

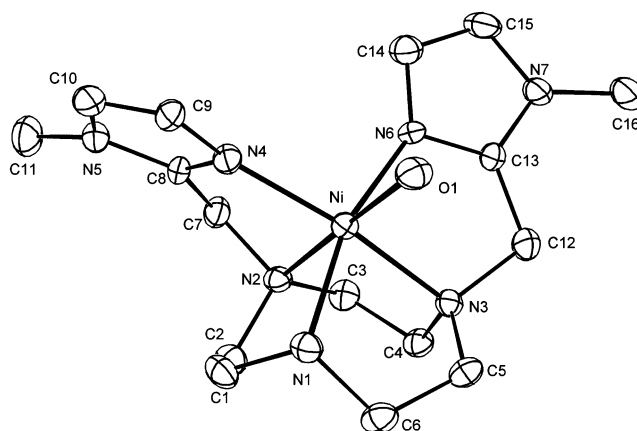


Fig. 3. A view of the $[\text{NiL}^2(\text{H}_2\text{O})]^{2+}$ cation in the structure of **4**.

Ni–N(N_3^-) distances differ significantly (Table 2), the shorter one lying *trans* to the longest of the Ni–N distances formed by the macrocycle nitrogens. The metal atom deviates by ≤ 0.16 Å from each of the three planes (hereafter ‘equatorial’ planes) of the idealized octahedron, each defined by four donor atoms mutually *trans* in pairs. In addition to the dimetal cations, the structure of **1** contains isolated PF_6^- anions.

The dimeric $[\text{Ni}_2\text{L}_2^2(\text{N}_3)]^{3+}$ cation of **5** (Fig. 2, Table 3) has a twofold axis normal to the bridging N_3^- anion. Each metal atom is coordinated by the five L^2 nitrogen donor atoms and one N_3^- nitrogen. The axis of the N_3^- ligand forms an angle close to 120° with the direction of the Ni–N(N_3^-) bond (Table 3). Similar values of the corresponding angles are formed by the two bridging anions in **1** (Table 2). The metal atom in **5** deviates from the equatorial planes by ≤ 0.15 Å. In addition to one half of the dimetal cation, the asymmetric unit of **5** contains one PF_6^- anion lying in general position and one half of a second PF_6^- anion, which lies in special position on a twofold axis.

The structure of **4** contains $[\text{NiL}^2(\text{H}_2\text{O})]^{2+}$ cations, BPh_4^- anions and (disordered) solvate ethanol molecules. The coordination in the monomeric cation (Fig. 3, Table 4) is provided by the five donor atoms of

the L² ligand and by the water oxygen. The conformation of the L² molecule is substantially similar to that attained in **5**, with the planes through the two methylimidazole groups forming closely related,

Table 4
Selected bond lengths (Å) and angles (°) for [NiL²(H₂O)]-[BPh₄]₂-C₂H₅OH (**4**)

Ni–N(1)	2.085(6)	Ni–N(4)	2.017(6)
Ni–N(2)	2.105(6)	Ni–N(6)	2.056(6)
Ni–N(3)	2.095(6)	Ni–O(1)	2.105(6)
N(1)–Ni–N(2)	83.3(2)	N(2)–Ni–O(1)	177.3(2)
N(1)–Ni–N(3)	83.2(2)	N(3)–Ni–N(4)	166.3(2)
N(1)–Ni–N(4)	97.0(2)	N(3)–Ni–N(6)	80.5(2)
N(1)–Ni–N(6)	163.6(2)	N(3)–Ni–O(1)	96.1(2)
N(1)–Ni–O(1)	94.0(2)	N(4)–Ni–N(6)	99.3(2)
N(2)–Ni–N(3)	84.2(2)	N(4)–Ni–O(1)	97.5(2)
N(2)–Ni–N(4)	82.3(2)	N(6)–Ni–O(1)	86.0(2)
N(2)–Ni–N(6)	96.8(2)		

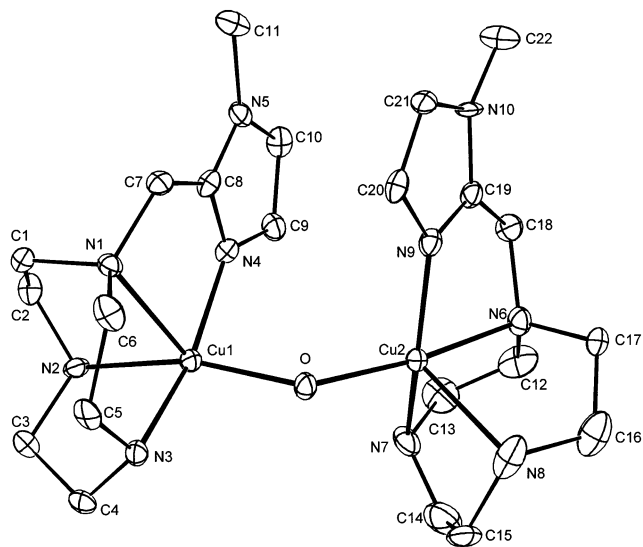


Fig. 4. A view of the [Cu₂L₂(OH)]³⁺ cation in the structure of **2**.

Table 5
Selected bond lengths (Å) and angles (°) for [Cu₂L₂(OH)][PF₆]₃ (**2**)

Cu(1)–N(1)	2.271(6)	Cu(2)–N(6)	2.085(6)
Cu(1)–N(2)	2.079(5)	Cu(2)–N(7)	2.005(7)
Cu(1)–N(3)	2.021(6)	Cu(2)–N(8)	2.200(7)
Cu(1)–N(4)	1.986(6)	Cu(2)–N(9)	1.989(6)
Cu(1)–O	1.913(4)	Cu(2)–O	1.925(5)
N(1)–Cu(1)–N(2)	80.5(2)	N(6)–Cu(2)–N(7)	82.1(3)
N(1)–Cu(1)–N(3)	84.2(2)	N(6)–Cu(2)–N(8)	83.8(3)
N(1)–Cu(1)–N(4)	80.0(2)	N(6)–Cu(2)–N(9)	82.3(2)
N(1)–Cu(1)–O	117.0(2)	N(6)–Cu(2)–O	168.9(2)
N(2)–Cu(1)–N(3)	83.8(2)	N(7)–Cu(2)–N(8)	83.5(4)
N(2)–Cu(1)–N(4)	96.0(2)	N(7)–Cu(2)–N(9)	155.8(3)
N(2)–Cu(1)–O	161.6(3)	N(7)–Cu(2)–O	95.1(3)
N(3)–Cu(1)–N(4)	164.0(3)	N(8)–Cu(2)–N(9)	112.9(3)
N(3)–Cu(1)–O	92.0(2)	N(8)–Cu(2)–O	106.6(2)
N(4)–Cu(1)–O	92.9(2)	N(9)–Cu(2)–O	96.6(2)
Cu(1)–O–Cu(2)	135.2(3)		

91.2(3)° **4** and 88.1(2)° **5**, dihedral angles in the two structures. However, if the angles formed by the above two planes and the plane through the macrocycle nitrogens in each structure are compared (43.6(3) and 52.8(3)° in **4**, 51.5(2) and 54.6(2)° in **5**), one of the angles in **4** is found to differ sensibly from the others. This is probably an effect of hydrogen bond interactions in **4** (see below). The metal atom in **4** deviates from the equatorial planes by ≤ 0.13 Å.

The mean values of the metal-donor atom distances in the nickel(II) derivatives (2.097 Å **1**, 2.086 Å **5**, 2.077 Å **4**) decrease regularly going from the dimeric cation with a double N₃[−] bridge to the monobridged one and then to the monomeric cation. Actually, part of this trend (from **1** to **5**) is substantially determined by the values of the Ni–N(N₃[−]) distances (Tables 2 and 3) and may result from comparatively high space demand within the coordination sphere by the charged ligands, particularly when there are two N₃[−] anions closely spaced, as in **1**. If only the Ni–N distances formed by the chelating ligands are considered, their mean values are found to be closely similar for the two N₃[−] derivatives (2.086 Å **1**, 2.084 Å **5**), both being only slightly smaller than the 2.089 Å mean found for the nickel(II) complex of the completely methylimidazol-functionalized macrocycle [16]. On the other hand, the 2.072 Å mean value of the Ni–N distances, all formed by L², in **4** is sensibly smaller than all of the former mean values. This could be due to the formation of (strongly bent) hydrogen bonds or related electrostatic interactions within the coordination sphere of **4**, between the water molecule and nitrogen atoms of L². Actually, the two candidate N atoms for such interactions, according to the PARST analysis [13] of the structure, the aminic N(1) and the methylimidazole N(4) nitrogen, form the shortest Ni–N bonds of the respective type in **4** (Table 4). Such interactions may also be responsible for the deviation, mentioned above, of the plane of a methylimidazole group in **4** (the one containing N(4)) from the expected orientation with respect to other planes in the structure.

The structure of **2** consists of dimetal [Cu₂L₂(OH)]³⁺ cations and PF₆[−] anions. Each of the two metal atoms (Fig. 4, Table 5) is five-coordinated by the four nitrogen donor atoms of the L¹ ligand and by the oxygen atom of the bridging OH[−] anion. The coordination geometry about each copper(II) atom is approximately square pyramidal, however with different arrangements of the two L¹ ligands. In the square pyramid about Cu(1) the donor atom in the apical position, N(1), is the macrocycle nitrogen bearing the pendant group, whereas in the Cu(2) polyhedron the apical atom, N(8), is one of the unsubstituted macrocycle nitrogens. As a consequence of this in the Cu(1) environment the methylimidazole plane is almost perpendicular to the basal plane of the square pyramid, with which it forms a 96.2(2)° dihedral

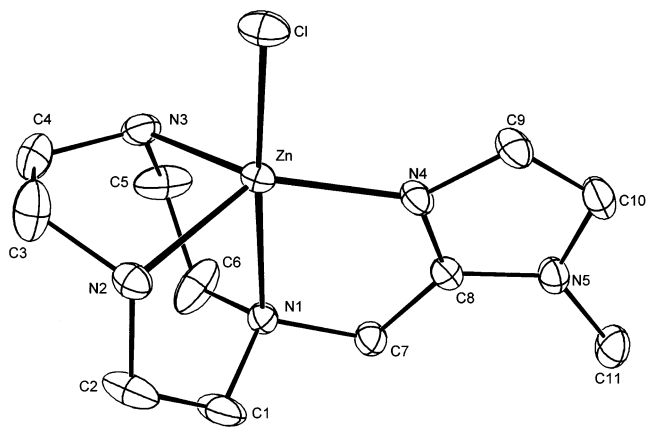


Fig. 5. A view of the $[\text{ZnL}^1\text{Cl}]^+$ cation in the structure of **3**.

Table 6
Selected bond lengths (Å) and angles (°) for $[\text{ZnL}^1\text{Cl}]\text{BPh}_4^-$ (**3**)

Zn–N(1)	2.346(3)	Zn–N(4)	1.982(3)
Zn–N(2)	2.079(3)	Zn–Cl	2.324(1)
Zn–N(3)	2.080(3)		
N(1)–Zn–N(2)	80.00(11)	N(2)–Zn–N(4)	132.79(13)
N(1)–Zn–N(3)	79.51(12)	N(2)–Zn–Cl	100.56(10)
N(1)–Zn–N(4)	77.24(11)	N(3)–Zn–N(4)	129.22(14)
N(1)–Zn–Cl	176.05(8)	N(3)–Zn–Cl	104.42(10)
N(2)–Zn–N(3)	85.4(2)	N(4)–Zn–Cl	99.72(9)

angle, whereas the angle between the corresponding planes in the Cu(2) environment measures $29.1(2)^\circ$. The metal atoms deviate by different amounts (Cu(1), $0.048(1)$ Å; Cu(2), $0.250(1)$ Å), each in the direction of the apical atom of its polyhedron, from the best plane through the four donor atoms forming the base of the respective square pyramid. The mean value of the metal to donor atom distances formed by Cu(1) is slightly longer, by 0.02 Å, than that of the distances formed by Cu(2), the difference being substantially due to the longer apical bond formed by Cu(1) (Table 5).

In the structure of **3**, formed by monomeric $[\text{ZnL}^1\text{Cl}]^+$ cations and BPh_4^- anions, the zinc(II) atom is five-coordinated by the four nitrogen atoms of the L^1 ligand and by the chlorine atom, with approximately trigonal bipyramidal geometry (Fig. 5, Table 6), which represents yet another coordination type within this series of compounds. The apical positions of the bipyramid are occupied by the chlorine and by one of the macrocycle nitrogens. This nitrogen, N(1), forms the longest bond to the metal ($2.346(3)$ Å) among those formed by nitrogen atoms in any of the present structures. The best line through the apical atoms and the metal is almost perpendicular to the equatorial plane, defined by N(2), N(3) and N(4), forming an angle of $2.0(1)^\circ$ with its normal. The zinc(II) atom deviates by $0.40(1)$ Å from that plane, in the direction of the chlorine atom. The arrangement of the dangling group

of the L^1 ligand in **3** differs considerably from those attained in **1** and **2**: with reference to the angle formed by the methylimidazole plane and the plane through the macrocycle nitrogens, this is found to measure $89.4(2)^\circ$ in **3**, whereas it is $50.8(1)^\circ$ in **1** and it possesses the $55.5(2)^\circ$ and $67.0(3)^\circ$ values in the two parts of the cation of **2**.

Overall, the present results point to considerable flexibility of the ligands, particularly of L^1 , which appears to comply easily with the geometrical preferences of specific metal ions, in combination with a variety of monodentate coligands. It is likely that even higher versatility will be exhibited by properly designed new ligands which may be synthesized according to the procedures outlined here and in the previous report [1].

4. Supplementary material

Crystallographic data (without structure factors) for the structural analyses have been deposited with the Cambridge Crystallographic Data Centre, as CCDC No. 127626 (**1**), 127629 (**2**), 127630 (**3**), 127627 (**4**) and 127628 (**5**). Copies of this information may be obtained free of charge from: The Director, CCDC, 12 Union Road, Cambridge CB2 1EZ UK, fax. +44-1223-336033.

Acknowledgements

We acknowledge financial support by the Italian Ministero dell'Università e della Ricerca Scientifica e Tecnologica.

References

- [1] M. Di Vaira, F. Mani, P. Stoppioni, *Inorg. Chim. Acta* 273 (1998) 151.
- [2] K. Wiegardt, U. Bossek, P. Chaudhuri, W. Herrman, B.C. Menke, J. Weiss, *Inorg. Chem.* 21 (1982) 4308. B.A. Hammer-shoi, A.M. Sargeson, *Inorg. Chem.* 22 (1983) 3554. B.A. Sayer, J.P. Michael, R.D. Hancock, *Inorg. Chim. Acta* 77 (1983) L63. K. Wiegardt, E. Schöffmann, B. Nuber, J. Weiss, *Inorg. Chem.* 25 (1986) 4877. U. Auerbach, U. Eckert, K. Wiegardt, B. Nuber, J. Weiss, *Inorg. Chem.* 29 (1990) 938. R. Ziesel, J.M. Lehn, *Helv. Chim. Acta* 73 (1990) 1149. C.J. Broan, K. Jankowski, R. Katak, D. Parker, *J. Chem. Soc., Dalton Trans.* (1990) 1738. I.A. Fallis, L.J. Farrugia, N.M. Macdonald, R.D. Peacock, *J. Chem. Soc., Dalton Trans.* (1993) 2759.
- [3] M. Di Vaira, B. Cosimelli, F. Mani, P. Stoppioni, *J. Chem. Soc., Dalton Trans.* (1991) 331. G. de Martino Norante, M. Di Vaira, F. Mani, S. Mazzi, P. Stoppioni, *J. Chem. Soc., Dalton Trans.* (1992) 361. M. Di Vaira, F. Mani, P. Stoppioni, *J. Chem. Soc., Dalton Trans.* (1994) 3739. M. Di Vaira, M. Guerra, F. Mani, P. Stoppioni, *J. Chem. Soc., Dalton Trans.* (1996) 1173. M. Di Vaira, F. Mani, P. Stoppioni, *J. Chem. Soc., Dalton Trans.* (1997) 1375.

- [4] G.R. Weisman, D.J. Vachon, V.B. Johnson, D.A. Gronbeck, J. Chem. Soc., Chem. Commun. (1987) 886. M. Studer, A. Riesen, T.A. Kaden, *Helv. Chim. Acta* 72 (1989) 307. N.W. Alcock, F. McLaren, P. Moore, G.M. Pike, S.M. Rae, J. Chem. Soc., Chem. Commun. (1989) 629. D.G. Fortier, A. McAuley, J. Chem. Soc., Dalton Trans. (1991) 101. G.A. McLachlan, G.D. Fallon, R.L. Martin, B. Moubaraki, K.S. Murray, L. Spiccia, *Inorg. Chem.* 33 (1994) 4663. D. Schulz, T. Weyhermüller, K. Wieghardt, B. Nuber, *Inorg. Chim. Acta* 240 (1995) 217. D. Ellis, L.J. Farrugia, D.T. Hickman, P.A. Lovatt, R.D. Peacock, *Chem. Commun.* (1996) 1817. L.J. Farrugia, P.A. Lovatt, R.D. Peacock, *Inorg. Chim. Acta* 246 (1996) 343.
- [5] M. Di Vaira, F. Mani, N. Nardi, P. Stoppioni, A. Vacca, J. Chem. Soc., Dalton Trans. (1996) 2679.
- [6] T.J. Atkins, J.E. Richman, W.F. Oettle, *Org. Synth.* 58 (1978) 86. K. Wieghardt, W. Schmid, B. Nuber, J. Weiss, *Chem. Ber.* 112 (1978) 2220.
- [7] R.G. Jones, *J. Am. Chem. Soc.* 71 (1949) 383.
- [8] N. Walker, D. Stuart, *Acta Crystallogr., Sect. A* 39 (1983) 158.
- [9] G.M. Sheldrick, SADABS, Program for CCD data absorption correction, University of Göttingen.
- [10] A. Altomare, M.C. Burla, M. Camalli, G. Cascarano, C. Giacovazzo, A. Guagliardi, G. Polidori, *SIR* 92, *J. Appl. Crystallogr.* 27 (1994) 435.
- [11] G.M. Sheldrick, SHELXL 93, Program for Crystal Structure Refinement, University of Göttingen, 1993.
- [12] C.K. Johnson, ORTEP II, Report ORNL-5138, Oak Ridge National Laboratory, Oak Ridge, TN, 1976.
- [13] M. Nardelli, *PARST*, *J. Appl. Crystallogr.* 28 (1995) 659.
- [14] H.D. Flack, *Acta Crystallogr., Sect. A* 39 (1983) 876.
- [15] L.J. Zompa, T.N. Margulis, *Inorg. Chim. Acta* 45 (1980) L263.
- [16] M. Di Vaira, F. Mani, P. Stoppioni, *J. Chem. Soc., Chem. Commun.* (1989) 126.